

Effect of Harmonic Currents on Semiconductor Fuse Ratings

R Wilkins
Consultant
Overdee, Rocky Lane
Heswall, Wirral, CH60 0BZ, UK

J. F. de Palma
Ferraz Shawmut
374 Merrimac Street
Newburyport, MA 01950, USA

C. Mulertt
Ferraz Shawmut
1, Rue Novel
FR-69100 Villeurbanne, France

Abstract—In power electronic applications, proximity and skin effects cause an increase in the resistance of fuse elements and possible unequal sharing of the total current between multiple parallel elements. In this paper the current density distribution is calculated for typical arrangements of fuse strips as a function of frequency, and methods of de-rating the fuse are discussed. The calculations are done using an equivalent wire-grid array method. De-rating factors are calculated for sinusoidal and some nonsinusoidal waveforms commonly found in power electronic applications. The implications for the design of semiconductor fuses for h.f. applications are also considered.

I. INTRODUCTION

The continuous current ratings of semiconductor fuses are determined in standard "type" tests with specified conditions. In real applications the conditions are always different, and it is well known that adjustments have to be made to allow for ambient temperature, size of connecting cables and any air cooling. Standard type tests are done at 50 or 60Hz, but in modern power electronic applications the frequency may be much higher. It is not widely recognized that this may require de-rating of the fuses. A recent paper [1] described problems caused by premature opening of fuses in the a.c. line inputs to adjustable-speed drives which drew unusually high harmonic currents.

Semiconductor fuse elements are made from multiple thin silver strips, and at higher frequencies skin effect causes crowding of the current at the edges of the strips [2]. More importantly, proximity effect causes an additional shift of current towards the return bus. The resulting non-uniform current distribution produces additional heating and a need for de-rating the fuse. The issue was first described by Howe & Jordan [3], who represented the fuse elements with an equivalent wire-grid array to calculate the magnitudes of skin and proximity effects. More recently Duong and others [4,5] used FEA and wire grid array methods to study the distribution of currents in strips with various orientations. Their calculations were also supported by experiments.

In this paper we will discuss alternative methods for de-rating fuses at elevated frequencies and also for some common waveshapes found in power electronic applications. Calculation of the current density distribution for typical arrangements of fuse elements is done using the wire grid array method. The method used is summarized in the Appendix.

II. TYPICAL CURRENT DENSITY DISTRIBUTIONS

Fig.1 shows 3 different arrangements of silver strips above a copper return bus. These are representative of some possible ways fuse element strips could be arranged in a semiconductor fuse. The strip and bus dimensions are 20 x 0.2mm and 30 x 2mm respectively. For cases (a) and (b) the strip spacing is 10mm, while for (c) the horizontal spacing is 22mm.

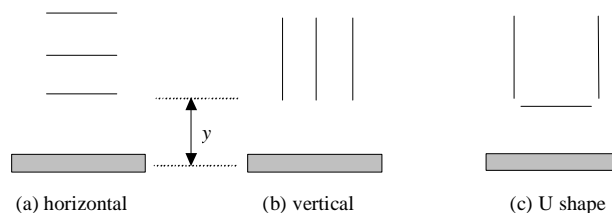


Fig.1 Different arrangements of three strips

Fig.2 shows the normalized distribution of the current density J in the strips, at 10kHz, with a distance to the return bus (y) of 20mm. J is plotted as a function of the distance along the strips, with $d=0$ at the strip center. For vertical strips, the left-hand side of the plot is the edge of the strip nearest to the return bus.

At this frequency skin effect is negligible with respect to the thickness of these strips, but very significant across their width.

For three horizontal strips - case (a) - the current in the strip at the bottom, nearest the return bus, is much greater than in the other two strips, and the distribution of J is symmetrical across the strip widths.

In case (b) the two outer vertical strips carry a slightly higher current than the center strip, due to the action of direct proximity effect within the group. However there is a large shift of current towards the return bus in all three strips, due to the inverse proximity effect.

For the U-shaped arrangement, the bottom strip carries significantly more current than the other two, and the distribution of J is symmetrical. The two vertical strips carry equal currents, and within them a small shift of current towards the return bus occurs.

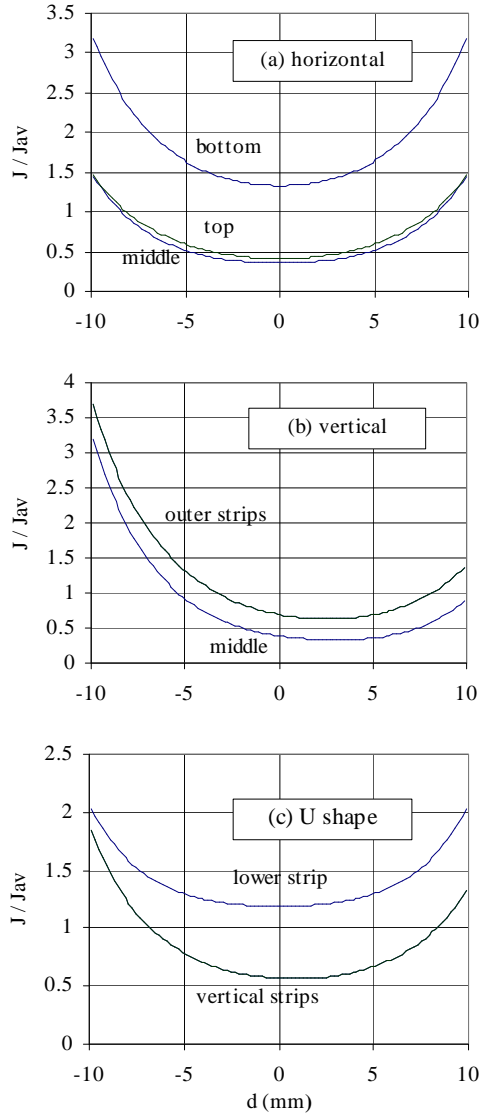


Fig.2 Normalized current density distributions
($y = 20\text{mm}$; $f = 10\text{kHz}$)

III. EFFECT ON FUSE RATING - SINUSOIDAL CURRENTS

Skin and proximity effects cause the total resistance and power dissipation in a fuse to increase, and at higher frequencies there is a need to reduce the ampere rating, to prevent excessively high temperatures. Two possible methods of de-rating the fuse are considered here.

A. De-rating on the basis of total power loss

In the standard type test at power frequency the total power produced in the fuse (P_N) is equal to $I_N^2 R_N$, where I_N is the nominal fuse rated current and R_N is the resistance at power frequency. If at higher frequency the resistance increases to R_H the nominal current rating needs to be reduced to I_H , to ensure that the total power does not exceed P_N . This is achieved by using de-rating factor F_P , where

$$F_P = \frac{I_H}{I_N} = \sqrt{\frac{R_N}{R_H}} \quad (1)$$

B. De-rating on the basis of maximum current per element

An alternative to (1) is to require that the current in the most heavily loaded strip does not exceed the highest value obtained in the standard type test. If we assume that, due to proximity effect, the current in the most heavily loaded element increases by a factor w_H at high frequency, then a de-rating factor F_C needs to be used, where

$$F_C = \frac{I_H}{I_N} = \frac{w_N}{w_H} \quad (2)$$

Normally skin and proximity effects at power frequency (50 or 60Hz) are negligible, so that the strips share the current equally, and $w_N \sim 1$. Fig.3 shows the de-rating factors F_P and

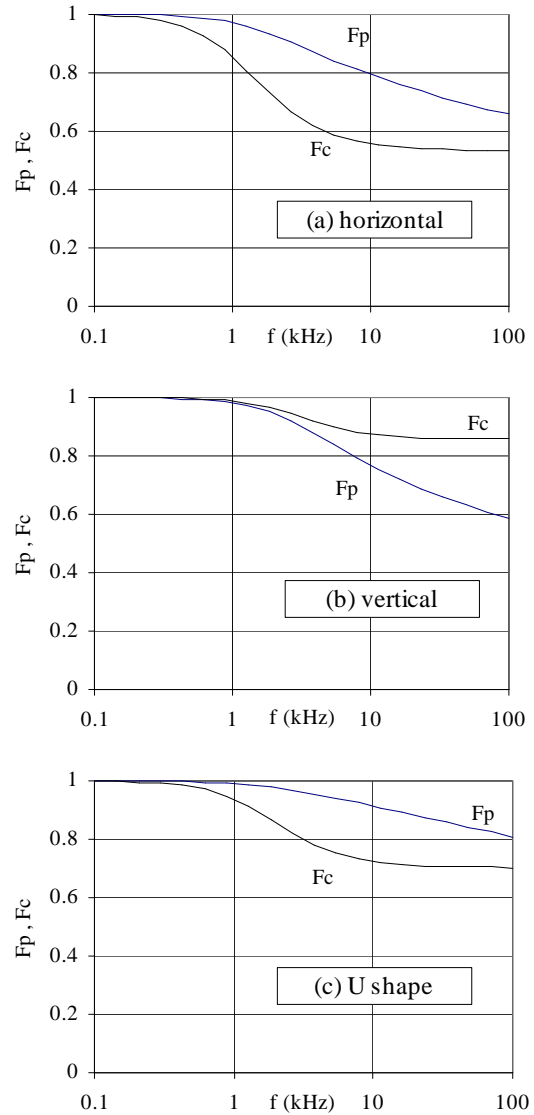


Fig.3 De-rating factors as a function of frequency

F_C for the three strip arrangements of Fig.1. F_P and F_C both decrease as the frequency increases, but are significantly different. In practice it would be necessary to use the lower value. For the horizontal strip arrangement, the de-rating factor F_C is much more significant (i.e. lower) than F_P . This is because of the strong shift in current to the bottom element, evident in Fig.1 (a). With three vertical strips, the reverse is true, because the difference in currents between the three strips is small. The dominant effect is the crowding of current towards the bottom edges of all three strips. For the U shape arrangement F_C is the dominant factor because of the shift of current to the bottom (horizontal) strip, but the effect is not as strong as case (a).

In all cases F_C tends toward a constant value for $f > 10\text{kHz}$. This is because the current distribution between the elements at high frequency becomes controlled by the distribution of the inductance external to the strips, which is constant. Nevertheless the resistance continues to increase with frequency, so that F_P continues to fall over the frequency range shown. Fig.3 shows that for single-frequency h.f. applications the required de-rating of a fuse can be very large, up to about 50%.

IV. DE-RATING FOR NONSINUSOIDAL CURRENTS

In most power-electronic applications the current waveform is periodic but nonsinusoidal. The r.m.s. current is given by

$$I_{RMS} = I_1 \sqrt{\sum p_H^2} \quad (3)$$

where I_1 is the fundamental component and p_H is the per-unit magnitude of the H' th harmonic. The total power produced in the fuse can be calculated from

$$P = \sum I_H^2 R_H = I_1^2 R_1 \sum p_H^2 q_H \quad (4)$$

where q_H is the per-unit harmonic resistance (R_H/R_1). If we require that the power in the application does not exceed the rated power P_N , and use (3) we obtain a de-rating factor F_P given by

$$F_P = \sqrt{\frac{R_N}{R_1} \cdot \frac{\sum p_H^2}{\sum p_H^2 q_H}} \quad (5)$$

For many applications the fundamental frequency of the application is the same as power frequency. In this case $R_N/R_1=1$.

Equation (4) results from the application of the principle of superposition, which is only valid for linear systems. In real fuses a non-linearity is introduced because the different parts of the strips are at different temperatures, and the resistivity of the metal is a function of temperature. So the method described here is an approximation based upon an assumption of constant temperature. (See section IV).

To derive F_C for nonsinusoidal application, assume that at each harmonic frequency the current in the most heavily loaded strip increases by a factor w_H . Using (3) this gives

$$F_C = w_N \sqrt{\frac{\sum p_H^2}{\sum p_H^2 w_H^2}} \quad (6)$$

To investigate the de-rating required for nonsinusoidal applications, four common current waveshapes have been used, with harmonic spectra as shown in Fig.4.

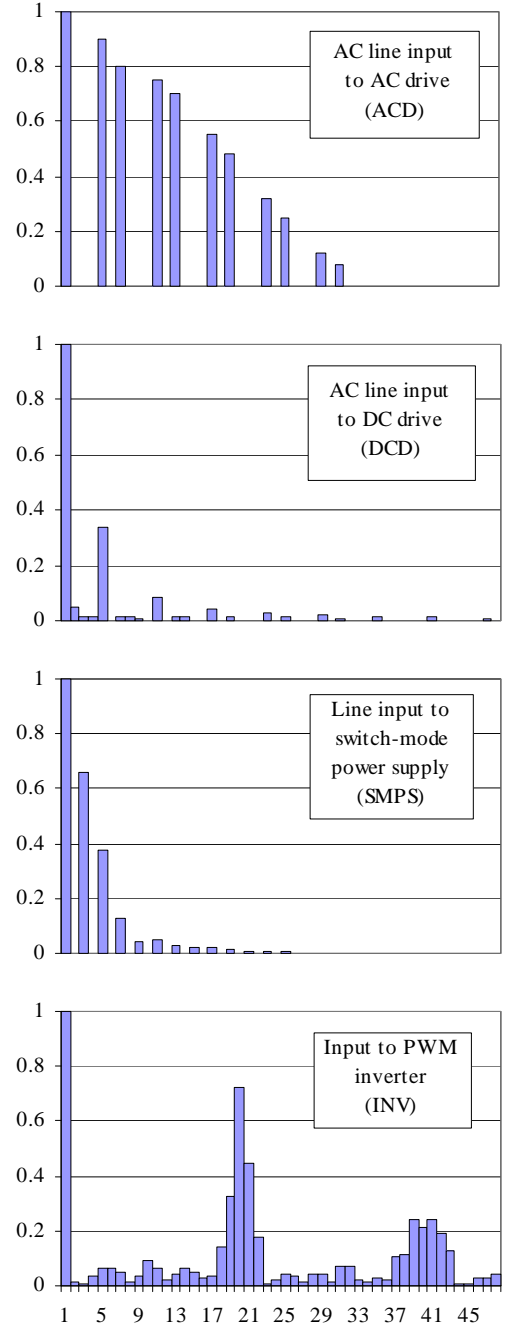


Fig.4 Spectra for 4 common current waveshapes

The spectra in Fig.4 correspond to the following circuits.

A. AC line input to PWM adjustable-speed drive (ACD)

This is a voltage-source inverter with the familiar "rabbit ear" current wave with two current pulses per half-cycle. It was the circuit which gave rise to the problems described in [1], although the drives in question were actually producing a much higher level of harmonics than normal.

B. AC line input to DC drive (DCD)

The dominant harmonics here are the 5th and the 11th.

C. AC line input to switched-mode power supply (SMPS)

This wave consists of a single pulse per half-cycle and contains few harmonics beyond the 11th.

D. Input to PWM inverter circuit (INV)

This is the waveshape of the current between the reservoir capacitor and the switching devices. The significant harmonics are clustered around multiples of the switching frequency, which in this case was 1 kHz.

Spectra A, B and C are based on data given in [6], while D was obtained from a PSpice simulation of a PWM inverter.

The de-rating factors F_P and F_C have been calculated for the spectra shown in Fig.4. This was done by calculating the current distribution for each harmonic frequency using the wire grid array method, from which the harmonic resistance and current shift factors p_H and w_H can be found. F_P and F_C are then obtained from (5) and (6). The results are shown in Fig.5, for the three different strip arrangements. Since the de-rating required in some cases is quite small, it is shown in Fig.5 as a required percentage reduction in nominal rating i.e. $(1-F_P) \times 100$ and $(1-F_C) \times 100$.

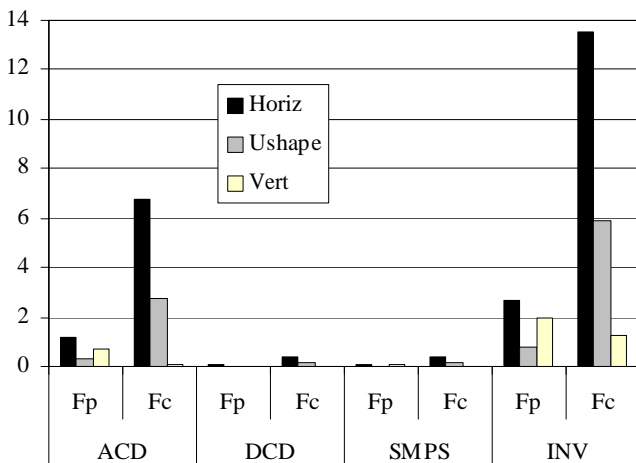


Fig.5 Percentage reductions in nominal current rating

For the d.c. drive and s.m.p.s. applications the required de-rating is negligibly small, less than 1%. However, a significant de-rating is necessary for the a.c. drive (~7%) and the inverter (~15%). These figures are for the worst case, i.e. three horizontal strips. In many applications, fuses are used as components and the fuse manufacturer has no control of how they are mounted in equipment, so de-rating for general application needs to be based on the worst case.

V. DISCUSSION

It should be emphasized that de-rating for harmonic currents is only one of the things which have to be considered when selecting a semiconductor fuse for a power electronic application. In selecting the required ampere rating, the influence of ambient temperature, size of connecting cables or busbars, cooling method, and the nature of any cyclic or surge overloads must be taken into account. In many cases the need for the fuse to withstand cyclic overloads will require a relatively large ampere rating, and this will be large enough to allow for any high-frequency effects.

The de-rating factors given here are intended to be used as a general indication of the order of magnitude of the influence of skin and proximity effects for a medium-sized fuse. In practice semiconductor fuses vary widely in size, with ratings from around 1A to several thousands of amperes, and with many different arrangements of the element strips. Real fuse strips also have rows of notches or holes which are used to control the arc voltage when interrupting short-circuit currents. The presence of these notches will modify the magnetic field distribution to small extent.

The wire grid array method assumes that the magnetic field is 2-dimensional, whereas in reality a fuse is a 3-dimensional object, and the results will be influenced by end effects. In a real application the distribution of current in the elements may also be affected by the presence of external magnetic fields due to other current-carrying conductors [9].

When a fuse is carrying current the temperature of the elements will be higher than the ambient temperature, and some element strips will be hotter than others. The resistance of these hotter strips will be higher, due to the positive temperature coefficient of resistivity of silver. At low frequencies the sharing of current is dominated by resistive effects, and the thermal effect will cause a shift of current away from the hotter strips to the parallel-connected cooler strips. This effect has been neglected in the analysis used here to calculate F_P and F_C . The thermal effect will be beneficial, as it will produce a slight shift of current away from the most heavily loaded strips.

However at high frequencies (above about 10kHz), the sharing of current is completely determined by the magnetic field distribution (distribution of external inductances) and the thermal effect will be negligible.

The results in sections III and IV have important implications for the design of semiconductor fuses for high-frequency applications such as the protection of IGBT inverters. However the design cannot be based solely on the minimization of skin and proximity effects. Another important requirement is the minimization of the insertion inductance of the fuse [7,8], so that a high switching di/dt is achievable without generating excessively high voltages. This requires a low-profile "flat-pack" fuse as shown in Fig.6. All elements strips in this design are at approximately the same distance from the return bus, minimizing the proximity effect. The flat-pack fuse needs to be kept small to minimize its insertion inductance, so the maximum ampere rating is limited. To achieve higher ampere ratings, these fuses can be connected in parallel, which has the added advantage of almost halving the total insertion inductance added to the circuit loop.

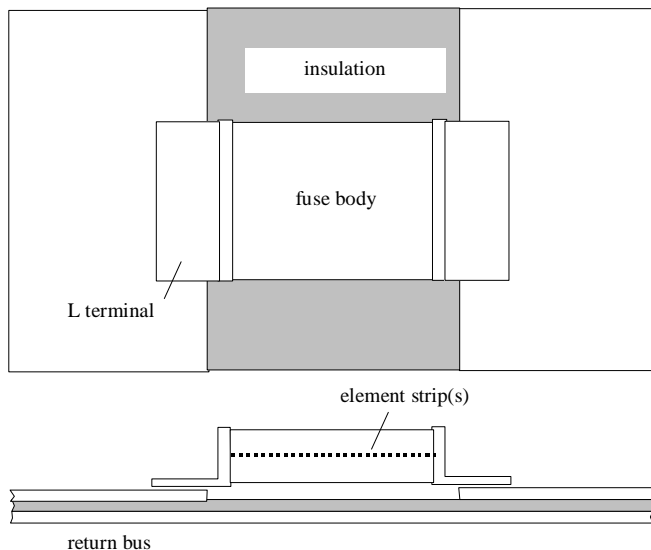


Fig.6 Minimization of proximity effect and insertion inductance

VI. CONCLUSION

Distributions of current density in a system of thin silver strips have been calculated using the wire grid array method, to estimate the de-rating required to allow for skin and proximity effects in typical semiconductor fuses.

For single-frequency h.f. currents a very large de-rating, up to 50% may be needed. Such applications are not common but are found for example in high-frequency inverters for induction heating. For most common power electronic applications the highest harmonic currents are usually below 1000Hz and de-rating of less than 10% is required. However fuses located at the input to PWM inverters carry high-frequency components of current, clustered around multiples of the switching frequency, and the required de-rating can be much higher.

In real applications skin and proximity effects are influenced by fuse design, thermal effects within the fuse elements, end effects, and the presence of other external magnetic fields. In critical cases the required de-rating can be determined by tests *in situ*.

REFERENCES

- [1] W. B. Leuschner and L. Ray, "Harmonic distortion contributes to accelerated fuse aging and premature failure" Presented at Power Quality 2000 conference, Boston, 3-5 Oct 2000.
- [2] P. Silvester, "Modal theory of skin effect in flat conductors", *Proc IEEE*, vol 54, No 9, Sept 1966, pp 1147-1151.
- [3] A. F. Howe and C. M. Jordan, "Skin and proximity effects in semiconductor fuselinks", *Fourth International Symposium on Switching Arc Phenomena*, Technical University of Lodz, Poland, 22-24 Sept 1981, pp 324-327.
- [4] S. Duong, C. Schaeffer, R. Deshayes and J.L. Gelet, "Distribution of high-frequency currents through the elements of a fuse", *Fifth International Conference on Electric Fuses and their Applications*, Technical University of Ilmenau, Germany, 25-27 Sept 1995, pp 229-235.
- [5] S. Duong, Y. Marechal, C. Schaeffer, C. Mulertt, F. Sarrus, and J.L. Gelet, "Electrothermal model of a fuse", *IEEE-IAS Annual Meeting Conf Record*, San Diego, Oct 1996, pp 1302-1308.
- [6] R. C. Dugan, M. F. McGranahan and H. W. Beaty, *Electric Power Systems Quality*, McGraw-Hill 1996.
- [7] R. Wilkins, H. C. Cline and E. J. Knapp, "Fuse protection of IGBT inverters", *PCIM98 Conference Proceedings*, Santa Clara, Nov 7-13, 1998, pp370-378.
- [8] J. L. Schanen, E. Clavel and J. Roudet, "Modeling of low inductive connections : the planar busbar structure", *IEEE-IAS Annual Meeting Conf Record*, Denver, Sept 1994, pp 1246-1250.
- [9] J.L. Gelet, D. Tournier and M. Ruggiero, "Evaluation of thermal and electrical behaviour of fuses in case of paralleling and/or high frequencies", *Sixth International Conference on Electric Fuses and their Applications*, IENG, Turin, Italy, 20-22 Sept 1999, pp 49-53.

ACKNOWLEDGMENT

Thanks are due to Jean-Claude Chenu for his help in the preparation of this paper.

APPENDIX

The calculations were done using a generalized version of the wire-grid array method, and the predictions were checked against published test data for several arrangements of single and multiple strips. The generalized version uses matrix methods which allow the fuse strips and return conductors to be represented as frequency dependent circuit elements. It is easily extended to model polyphase systems.

Fig.7 shows a number of conducting strips sharing a total a.c. current \mathbf{I} , which returns to the supply via a return bus.

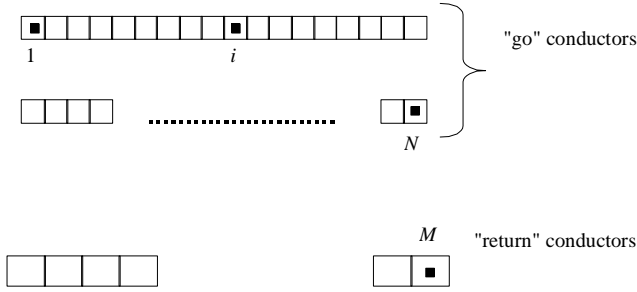


Fig.7 Subdivision of strips into wire subconductors.

The strips and return bus are subdivided into N and M rectangular sub-conductors (wires) respectively. This can be represented [8] by the circuit shown in Fig.8.

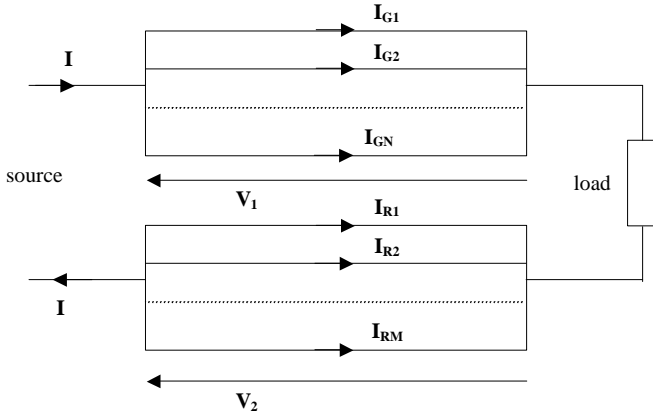


Fig.8 Equivalent circuit

For unit length of the conductors this can be modeled by the partitioned transmission-line matrix equation

$$\begin{bmatrix} \mathbf{V}_G \\ \mathbf{V}_R \end{bmatrix} = \begin{bmatrix} \mathbf{Z}_{GG} & \mathbf{Z}_{GR} \\ \mathbf{Z}_{RG} & \mathbf{Z}_{RR} \end{bmatrix} \begin{bmatrix} \mathbf{I}_G \\ \mathbf{I}_R \end{bmatrix} \quad (7)$$

\mathbf{I}_G is the $N \times 1$ vector of currents in the "go" group
 \mathbf{I}_R is the $M \times 1$ vector of currents in the "return" group
 \mathbf{V}_G is an $N \times 1$ vector with all elements equal to \mathbf{V}_1
 \mathbf{V}_R is an $M \times 1$ vector with all elements equal to \mathbf{V}_2

The $N \times N$ submatrix \mathbf{Z}_{GG} corresponds to the "go" group of wires and the $M \times M$ submatrix \mathbf{Z}_{RR} to the "return" group. There are $(N+M+2)$ complex unknowns in this system, the $N+M$ currents in the wires and the voltage drops \mathbf{V}_1 and \mathbf{V}_2 . The set (7) provides $N+M$ equations and two more are obtained from the requirement that the currents in each group must sum to the total (known) current \mathbf{I} i.e.

$$\sum_{i=1}^N \mathbf{I}_{Gi} = \mathbf{I} \quad \text{and} \quad \sum_{i=1}^M \mathbf{I}_{Ri} = -\mathbf{I} \quad (8)$$

The diagonal elements of the impedance matrix \mathbf{Z} are the self-impedances

$$z_{ii} = R_{ii} + \frac{j\omega\mu_0}{2\pi} \ln \frac{D}{r_i'}$$

where

$$R_{ii} = \text{resistance of wire } i = \rho_i / A_i$$

$$A_i = \text{cross-sectional area of wire } i$$

$$r_i' = \text{geometric mean radius of wire } i$$

D is the distance to a hypothetical remote return conductor, which may be set to an arbitrarily large value. This hypothetical conductor carries no current but must be included, as the self-inductance of an isolated conductor is infinite [2].

The off-diagonal elements of \mathbf{Z} are the mutual inductive reactances

$$x_{ij} = \frac{j\omega\mu_0}{2\pi} \ln \frac{D}{d_{ij}}$$

where d_{ij} is the distance between wires i and j .

The solution procedure is as follows. First \mathbf{Z} is inverted to give

$$\begin{bmatrix} \mathbf{I}_G \\ \mathbf{I}_R \end{bmatrix} = \begin{bmatrix} \mathbf{Y}_{GG} & \mathbf{Y}_{GR} \\ \mathbf{Y}_{RG} & \mathbf{Y}_{RR} \end{bmatrix} \begin{bmatrix} \mathbf{V}_G \\ \mathbf{V}_R \end{bmatrix} \quad (9)$$

Now apply (8). Adding the first N currents and then the next M currents we obtain the 2×2 matrix equation

$$\begin{bmatrix} \mathbf{I} \\ -\mathbf{I} \end{bmatrix} = \begin{bmatrix} \mathbf{A} & \mathbf{B} \\ \mathbf{C} & \mathbf{D} \end{bmatrix} \begin{bmatrix} \mathbf{V}_1 \\ \mathbf{V}_2 \end{bmatrix} \quad (10)$$

where \mathbf{A} is the sum of all the elements in \mathbf{Y}_{GG}

\mathbf{B} is the sum of all the elements in \mathbf{Y}_{GR} , and so on.

Solving (10) gives the voltages \mathbf{V}_1 and \mathbf{V}_2 . Substitution in (9) then gives the currents in the wires.

The total power produced in the strips is calculated from

$$P = \sum_{i=1}^N |\mathbf{I}_{Gi}|^2 R_{ii}$$

To obtain the current distributions for the systems of Fig.1 each strip was divided into 100 square subconductors and the return bus into 15, giving a 315×315 matrix, and D was set to 100m. The results were checked by comparison with the test data given in [4]. A comparison was also made with the results given in [2], for a single isolated strip, by moving the return bus a large distance away. In all cases good agreement with test data was obtained.